

Reliability assessment of tidal stream energy: significance for large-scale deployment in the UK

F. Khalid, P. R. Thies & L. Johanning

College of Engineering, Mathematics and Physical Sciences, University of Exeter, Renewable Energy Group, Cornwall Campus, Penryn TR10 9FE, United Kingdom

ABSTRACT: The UK has ambitious plans to harness its available tidal stream resource, estimated at 95TWh/year by The Crown Estate (2013). The economic viability of large-scale deployments will be largely governed by aspects of plant availability, including reliability. Using available information on environmental parameters of (pre-) consented sites across the UK, this paper explores subassembly target reliability levels for tidal stream devices. Reliability models of devices are investigated to establish the influence of environmental site conditions with regard to underlying subassembly failure rates and target reliability levels. Hence, a reliability-focussed perspective on the planned deployments is presented.

Keywords: *tidal stream energy, failure rate adjustment, metocean parameters, reliability target levels*

1 INTRODUCTION

With the potential to supply a quarter of UK's electricity demands, tidal stream technology is a growing sector (TCE, 2012). The world's first tidal stream array is under construction at Pentland Firth, Scotland placing the UK at the forefront of the industry. However, to allow the industry to be commercially viable, a levelised cost of energy (LCoE) of 10-20p/kWh by 2020 and 5-8p/kWh by 2050 (Energy Technologies Institute, 2015) is envisaged as an industrial target. A significant contributor to LCoE is annual energy production which is highly dependant on the available resource at site and device performance metrics of reliability and availability (SIO, 2014). Numerous studies by the Energy Technologies Institute (ETI, 2015), Strategic Initiative for Ocean Energy (SIO, 2014) and CATAPULT (2015) discuss the significance of device availability levels to improve the momentum of the industry growth. This paper explores how differences in environmental site conditions and associated target reliability affect the expected availability levels.

1.1 *Reliability of Tidal Energy*

According to ISO8402 (ISO, 1986), reliability is 'the ability of an item to perform a required function, under given environmental and operational conditions and for a stated period of time.' A tidal stream device (TSD) continues to perform its function, i.e. generate

electricity, until a 'failure' occurs. IEC 50 standards (IEC, 1990) define a failure as 'an event when a required function is terminated.' An important statistical measure required for reliability assessment is the failure rate. It is calculated as the ratio of the number of failures to the total observed time.

There is a lack of publicly available, field failure data for reliability calculations since the industry is at a rather early stage of development so the device developers not only have limited experience but also, prioritise confidentiality to maintain competitive advantage. The offshore oil and gas industry was at a similar stage in the past: data confidentiality was crucial. However, soon the industry realised the benefits of knowledge sharing for all involved parties and initiated the Offshore Reliability Database (OREDA) project (OREDA, 2002).

The launch of the small scale Reliable Data Acquisition Platform for Tidal (ReDAPT) project (RenewableUK, 2013) along the lines of OREDA was supported by the ETI using a 1MW Alstom Tidal Generation device. Findings of the ReDAPT project pertinent to this study include reaffirmation of the hypothesis that the challenges of operating in intense tidal regimes have been underestimated, and the investigation of device performance indicators like reliability in offshore conditions is paramount (ETI 2015).

Failure rate models require data from individual devices with particular operating conditions to esti-

mate point values for reliability, therefore, a statistically robust database is vital for precision. However, the absence of technology specific data for TSDs has led to extrapolations of device and operational environment using expert knowledge (Delorm & Tavner, 2010). The Military Handbook (US Military, 1949) can be credited for devising this simple method of multiplication of base failure rates with empirical factors to calculate site specific failure rates. This method introduces high degrees of uncertainties in Reliability Assessment results so they do not numerically represent the measured field reliability but rather provide a generic estimate.

1.2 Influence of Metocean parameters on Reliability

There exists a nonlinear dependence of power and device output on tidal stream velocity. Noticeably, marine current resource at locations with currents exceeding 2 m/s is a relatively intense renewable energy source relative to solar and wind (Fraenkel, 2002).

Past analyses of generic structural failures in the seas off Northwestern Europe report increased failures during storms in the late autumn and winter (Kettle, 2003). If correlated with oceanographic data, it can be seen that greater wave heights and current speeds are seen during these months. Therefore, environmental factors are expected to play a role in failure rate calculations, however, this has not been quantified for tidal stream technology in the literature to date.

1.3 Subassembly Reliability Targets

A common challenge in reliability engineering is translating reliability targets at the system level to requirements at the subassembly level. There is a lack of field and long-term deployment experience with tidal energy technologies to achieve robust reliability targets. For a given subassembly, failures and downtimes gradually decrease with the increased maturity of a given turbine model (Faulstich & Hahn, 2009) due to increased experience of manufacturers and operators. Each new deployment adds to the experience of offshore conditions and this information is used to make informed decisions regarding site-specific device manufacturing and effective O&M routines for optimised reliability targets (Faulstich et al. 2009b).

2 METHODOLOGY

This paper aims to quantify subassembly reliability levels for a tidal stream turbine deployed at various locations in the United Kingdom Continental Shelf (UKCS) to account for influences of metocean parameters on subassembly failure rates and consequence for target reliability levels.

2.1 Choosing Representative Sites for deployment

2.1.1 Data Sources-Metocean and UKCS lease sites

Using methodology similar to Carbon Trust & Black and Veatch (2011) and publicly available data for metocean parameters, four representative sites were chosen for TSD deployment in the UKCS. For tidal parameters, a Proudman Oceanographic Laboratory (POL) model with a resolution of $1/60^\circ$ latitude by $1/40^\circ$ longitude and for wave, a MetOffice model with 7 year data of spatial resolution 12 km is used by the Atlas of UK Marine Renewable Energy Resources (ABPmer, 2008). Figure 1 shows the data set that was used highlighting the abundance of annual average tidal power available in the UKCS. For wind, the Atlas' mesoscale model, with resolution of $1/9^\circ$ latitude and $1/6^\circ$ longitude, provides a depiction of metocean conditions for creating appropriate adjustment factors.

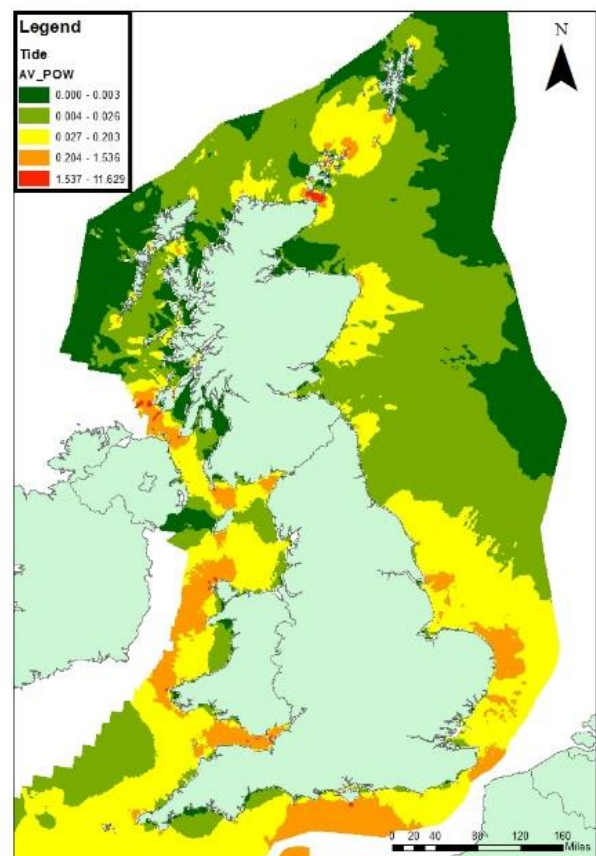


Figure 1. Tidal Stream resource in UKCS (adapted from ATLAS of UK marine renewable energy resources)

Additionally, a tidal lease site dataset showing the extent of live tidal agreements in the UK waters compiled by The Crown Estate (TCE, 2014) was used. These sites are a part of Round 1 and 2 announced by The Crown Estate in 2010 and 2014, respectively.

The aforementioned shape files for tidal, wave and wind parameters for UKCS along with the leased tidal sites were imported, aligned and analysed with ArcGIS.

2.1.2 Data Processing

The main aim of this process was to attribute site-specific wind, wave and tidal characteristics to the tidal lease sites using ArcGIS. Each site is given an average of the numeric attributes of the data polygons in the wave/tidal/wind shape files that intersect it. This creates new layers with wind, wave and tidal parameters appended to the attribute table of the lease sites. The extended tables from ArcGIS were exported and analysed with the following metocean and lease site data specifications:

Table 1. Compiled metocean and lease site data from The Crown Estate and ATLAS of UK marine renewable energy resources

Lease Sites	Metocean Parameters		
	Wind	Wave	Tidal
Property Name	Annual Wind Speed at 100m	Annual Significant Wave Height	Average Spring Peak Current
Lease Type	Annual Power Density at 80m	Average Annual Wave Power	Average Neap Peak Current
Tenant Name		Annual Winter Significant Wave Height	Average Annual Power

TSD lease sites must be located in areas of high resource, that is, powerful sea currents. Near shore lease sites include regions where flows are concentrated such as straits between islands. However, the POL model captures the tidal stream current variation in these areas poorly. Once plotted, it is noticeable that the density of lease sites in areas of low tidal power is high. This highlights the significance of acquiring high resolution model or field data to attain a better understanding of the leased sites for tidal turbine deployment through other sources like Admiralty Charts.

In order to complete the dataset, additional literature research for the tidal parameters of the lease sites was conducted. For wind and wave data, however, attributes of the nearest polygon were associated to the lease site.

2.1.3 Metocean reliability influences at Representative Sites

Owing to the influence of metocean parameters of wave and tides on TSD reliability, lease sites are classified into four groups to calculate the parameters for the four representative sites for TSD deployment. Only sites with annual average power density in excess of 1kW were included in the analysis as shown in Figure 2. This is because the low resource (<1kW) associated to other lease sites can be attributed to the crude dataset which might skew the results, if included. The retained sites were classified with respect to optimum peak spring tidal velocity (v_T) (Douglas et al. 2008) and the winter significant wave height

(H_s) characteristics. The former is significant for the economic viability of TSDs and the latter for the determination of an appropriate maintenance regime, as well as an indication of additional wave loading.

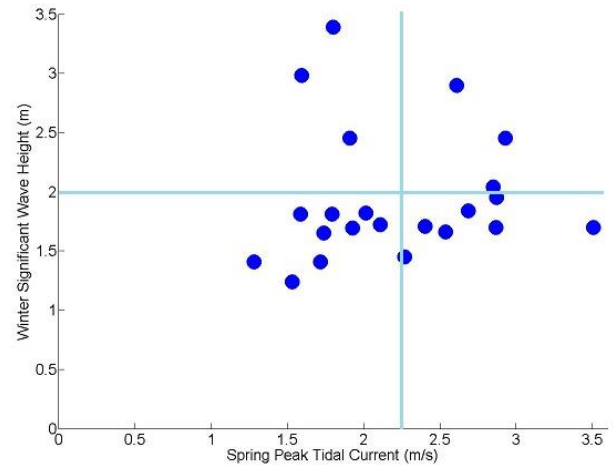


Figure 2. Metocean parameters for analysed TCE lease sites in UKCS.

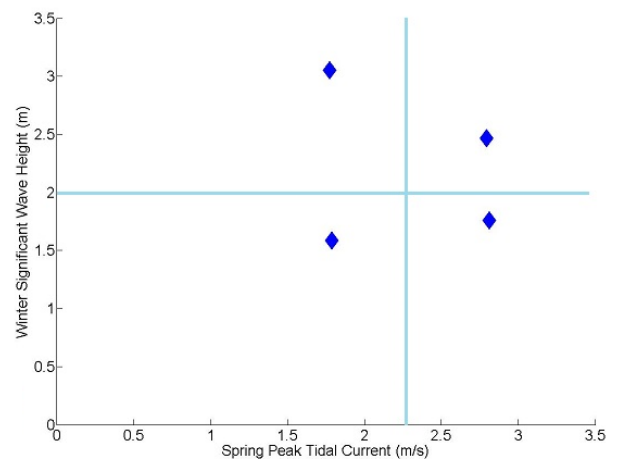


Figure 3. Metocean parameters for representative TSD lease sites in UKCS.

Table 2. Metocean parameters for TSD representative sites.

Lease Site	Wave - H_s (m)	Tidal - v_T (m/s)
Representative Site I (RI)	>2.0	>2.25
Representative Site II (RII)		<2.25
Representative Site III (RIII)	<2.0	
Representative Site IV (RIV)		>2.25

Calculating the average metocean parameters for each representative site yields the characteristic metocean parameters for each site as described in Figure 3. As seen in Table 2, the representative sites in the first and fourth quadrant, RI and RIV respectively, are located in areas of high tidal resource with peak tidal currents of 2.8m/s. Additionally, RI and RII (quadrant 2 and 3, respectively) are expected to have

relatively lower reliability than RIII and RIV due to the unfavourable H_s parameters of upto 3.1m prevalent during winters. Therefore, RI and RIV are attractive sites for TSD deployment. RIV is attractive for TSD deployment due to high reliability but has the disadvantage of a lower resource potential whereas RI maybe categorised as a location with high resource potential and consequently low reliability.

2.2 Reliability Modelling

2.2.1 Device Profile

Tidal stream technology is a very dynamic industry at the moment: new devices and new processes are continually developed and demonstrated, making it difficult to determine which device concepts will eventually be deployed at the farms in the UKCS. For the scope of this project, the AR-1500 by Atlantis Resources Corporation is chosen to demonstrate the influence of metocean parameters on reliability. This is due to its prospective deployment at Meygen Inner-Sound (the world's first TSD array) and the success of its predecessor in the ReDAPT project. At a rated capacity of 1.5MW, this system operates as a geared device with pitching blades, full nacelle yaw rotation capability (Meygen, 2011) and 1300 tonne gravity base to withstand loads in the highly energetic deployment locations.

2.2.2 Failure data mining for single TSD

Based on methodology from literature (Thies et al. 2009), it can be seen that reliability calculation involves allocation of a probabilistic distribution of industry-specific or adjusted failure statistics (λ_C) to individual subassemblies. Due to the absence of TSD data, surrogate data from greater than 10-years' onshore wind turbine failure rate databases (Tavner, 2006; Tavner, 2008) was used to provide annual base failure rates (λ_B) for the TSD subassemblies.

Table 3. TSD subassembly failure rate database from onshore wind and oil and gas industry.

Subassembly	λ_B [1/annum]	Source
Shaft & Bearings	0.03375	Tavner et al. 2006 Tavner et al. 2008
Brake	0.0875	
Generator	0.17125	
Parking Brake	0.0275	
Electric	0.38875	
Blade	0.4225	
Yaw System	0.13625	
Pitch mechanism	0.1575	
Gearbox	0.17875	
Other	0.31375	
Hydraulics	0.13375	
Electronics+Sensors/Control	0.38675	

Tripod Steel Gravity Based Foundation	OGP, 1.09E-03 2010
---------------------------------------	--------------------

The failure rate data for the anemometer was disregarded and the failure rate for the tripod steel gravity based foundation for UKCS Fixed Units installations (OGP, 2010) was introduced. The resulting λ_B for the device was calculated at 2.4 failures/annum with subassembly failure rates recorded in Table 3.

2.2.3 Limitations of TSD base failure rate database

Surrogate data from an onshore wind turbine (WT) is suitable for use in the reliability model of a TSD due to the similarity in working principle of both devices. Both devices extract kinetic energy from fluids using similar subassembly configuration. However, the operating conditions and the consequent reliability of an onshore wind turbine and a TSD are fairly different.

The most discernible cause for this is the difference in the properties of the resource fluids. Water is over 800 times denser than air and therefore has a higher power intensity than wind flows. This exposes the TSDs to much higher loads relative to WTs. Additionally, the presence of waves introduces increased turbulence to the operating environment of a TSD. Marine biofouling is also expected to have a greater effect on the reliability of a TSD compared to aerial fouling in a WT. Furthermore, since a TSD is fully submerged, it is more prone to corrosion-related failures than a WT.

The different media, wind and water, that the onshore wind turbine and TSD are deployed in, respectively, have a different effect on the individual subassemblies. The complexity of the loading on a TSD is increased by the fatigue loading on the pitch, yaw and shaft by wave-induced loading. In addition to the high power intensity of water, large fluctuations in flow velocity attributed to waves leads to high thrusts which may lead to blade failure. Also, the probability of blade damage due to collision with marine life may be different relative to damage induced in WTs. However, failures due to lightning are not likely to happen for a TSD. Scour and fatigue for the foundations of a TSD are noticeably higher than those for a WT. Similarly, failures due to corrosion are more likely to occur in the structure and bolts of a TSD. Also, failures of seals in a TSD might lead to leakages in the nacelle which may cause immediate failure of major drive train components.

To adjust the base failure rates from the onshore wind turbine data for use in TSD reliability assessment, an environmental adjustment is performed to account for the additional failure mechanisms for an offshore, submerged device.

2.2.4 Environmental adjustment of λ

The Military Handbook (MIL-HDBK) uses a 'parts stress analysis' method to effectively translate failure

rates from the data collection environment to application environment. Adjustment of base failure rates of electric components is performed using Equation 1 (US Military, 1949):

$$\lambda_C = \lambda_B \times \pi_E \times \pi_{FM} \times \pi_{DS} \quad (1)$$

Whereby,

λ_C = Adjusted failure rate of the component

λ_B = Base failure rate

π_E = Environmental adjustment factor

π_{FM} = Failure mode adjustment factor

π_{DS} = Data source uncertainty factor

This methodology was employed for this research project to determine site specific TSD subassembly failure rates from onshore wind failure data. Firstly, the impact of wave and tidal conditions on subassembly reliability was assessed individually. Both influencing factors were then used to devise an environmental adjustment factor for each representative site. The resulting device and subassembly failure rates were then calculated using Equation 1.

Site specific v_T was normalised against the offshore wind failure rate (Carroll, 2015) to calculate π_T , the adjustment factor for a representative site based on the tidal regime. This was done using Equation 2, where v_{Tmax} is the maximum velocity from the v_T array.

$$\pi_T = v_T/v_{Tmax} \times 8.3 \quad (2)$$

Alternatively, the ground benign to naval submarine adjustment factor from the Military Handbook could be used to provide an estimate of π_T . However, the similarity between the structure and function of offshore wind turbines and TSDs supersedes the relevance of the MIL-HDBK which is primarily used for military electrical equipment. Nevertheless, to account for the influence of wave parameters on reliability, the winter H_s was correlated with the adjustment factors in the MIL-HDBK to calculate π_w using Equation 2. H_{smax} is the maximum value of the H_s array.

$$\pi_w = H_s/H_{smax} \times 1.58 \quad (3)$$

This double consideration of factors may lead to a rather conservative estimate of reliability and consequently overestimate the difference in reliability at the deployment sites. Therefore, the resulting figures must not be taken as point estimates but rather as illustrators of reliability.

Site specific adjustment factors, π_E , for the representative sites were calculated as the product of π_w and π_T . These adjustment factors, shown in Table 4, were then applied to individual subassemblies to calculate the resultant subassembly failure rate to be fed into the model. The table also shows the annual device failure rates for a base failure rate of 2.4 for all

four sites. Figure 4 summarises the resource and reliability characteristics of the four representative sites. This paper will compare and contrast the reliability levels for devices deployed at RI and RIII to explore the balance between reliability and resource for tidal stream technology.

Table 4. Spring Peak tidal current, significant wave height (winter), adjustment factors and adjusted device failure rates for representative sites.

Site Name	π_E			
	RI	RII	RIII	RIV
v_T (m/s)	2.80	1.78	1.79	2.81
π_T	8.26	5.24	5.28	8.3 *
H_s (m)	2.47	3.05	1.58 **	1.76
π_w	1.28	1.58	0.82	0.91
π_E	11	8	4	8
Device λ (1/annum)	27	20	10	20

* (Carroll et al. 2015); ** (US Military, 1949)

		Resource	
		High	Low
Reliability	High	RIV	RIII
	Low	RI	RII

Figure 4. Resource-Reliability comparison of representative sites.

2.2.5 Modelling the tidal energy Representative Sites

Reliability block diagrams were built in BlockSim with statistically independent subassembly blocks which reflect the logical behaviour of the system. After connecting the blocks in the system configuration, associated failure rates are used to compute system reliability (Rausand & Høyland, 2003). When allocating lifetime failure characteristics to the subassemblies, the 2 parameter Weibull distribution was used but due to limited data regarding the influence of aging on the device, $\beta = 1$ was used for all subassemblies. The failure statistic required for reliability calculations is the Mean Time to Failure (η) defined as the average time between the start of an operational phase and the failure occurrence. To calculate hourly η , the following formula is used:

$$\eta = \frac{8760}{\lambda} \quad (4)$$

Device models for RI and RIII were created using system configuration as shown in Figure 5 with associated system reliability calculated as follows:

$$R_{System} = +II R_{Subassembly} \quad (5)$$

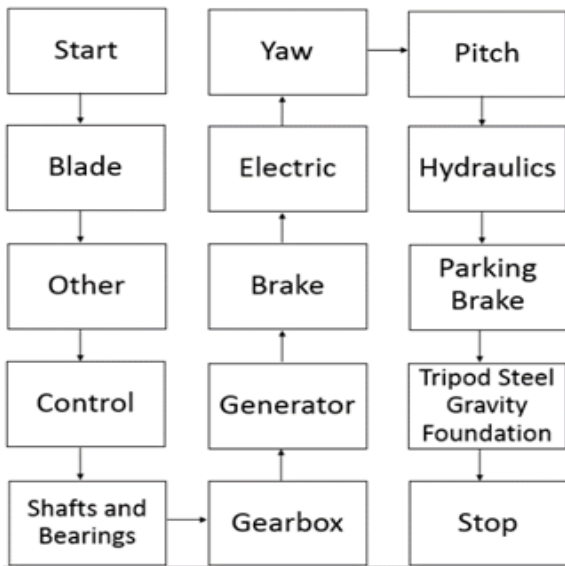


Figure 5. System configuration for AR-1500, the modelled TSD.

The reliability analysis is solely based on failure characteristics of the components; details of repair and restoration are not introduced in the analytical model of the device. An additional limitation is the assumption of a constant failure rate for the sub-assemblies. This discounts the negative influence of aging on device performance. Figure 6 shows the system reliability for AR-1500 deployed at RI and RIII. The considerable difference in device reliability levels can be directly attributed to the variation in metocean parameters at the deployment site.

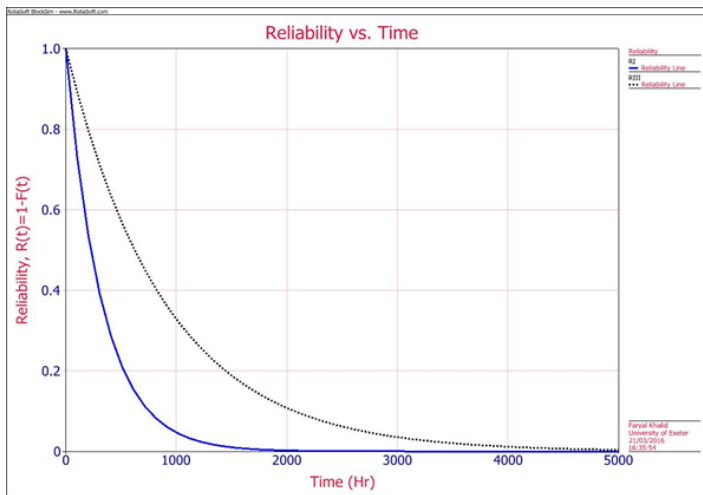


Figure 6. Comparison of reliability levels of RI and RIII.

2.2.6 Target Reliability at subassembly level

BlockSim provides three methods to allocate target reliability at subassembly levels: equal allocation, weighted reliability allocation and cost optimisation allocation. Using the Weighted Allocation Analysis method in BlockSim 8, the improved failure rates are derived based on weighting factors. With sufficient industrial data, these factors must be determined by analysing the complexity, technological limitations and maturity of the subassembly design. However, for the scope of this study, the allocation analysis was correlated with the contribution of each subassembly

to the failure rate. Weightings were allocated to each subassembly in the range of 5 to 80; an increased value represents a mature technology, for which sub-assembly reliability cannot be easily improved.

3 RESULTS

3.1 Temporal parameters for setting reliability targets

Calculation of point reliability levels for RI at 1, $\frac{1}{2}$, $\frac{1}{4}$ and $\frac{1}{12}$ yearly levels allows us to explore the effect of 'no maintenance windows' on the sub-system reliability estimates.

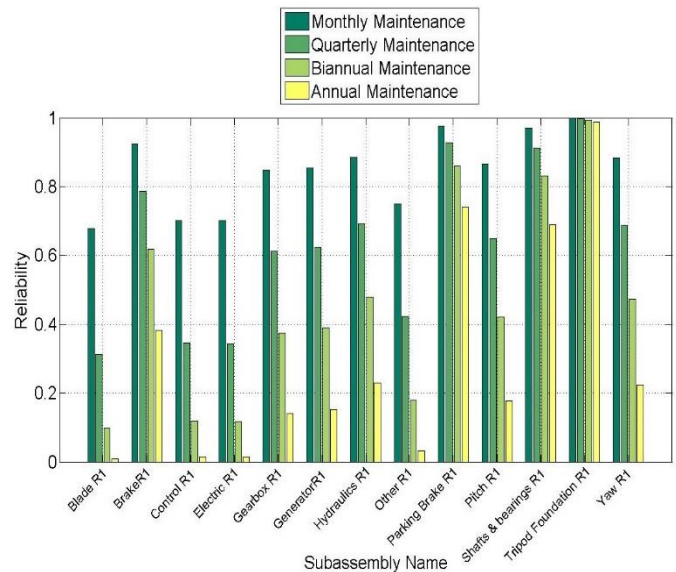


Figure 7. Subassembly reliability levels for monthly, quarterly, biannual and annual maintenance regimes.

Figure 7 shows subassembly reliability levels for RI achieved at annual, biannual, quarterly and monthly levels. It can be seen that reliability falls below 50% for certain subassemblies after 3 months so a long term analysis for device reliability was not conducted and a quarterly maintenance regime seems most feasible. For the available dataset, it can be seen that with a reliability level of 0.3 after 2190 hours, the blades are the least reliable subassembly. In contrast to this, the tripod steel gravity base is highly reliable likely due to the use of different industry datasets for the failure rate derivation.

3.2 Subassembly Target Reliability Levels

Figure 8 and 9 compare the actual reliability of subassemblies to the target reliability levels for achieving 65 and 95 percent device reliability at RI and RIII, respectively, after 3 months of operation. The maximum required improvement at subassembly level ranges from 0 to 3.2 times for RI and 0 to 1.5 times for RIII. The expected reliability improvement relies heavily on the weightage provided to individual subassemblies, and consequently the subassembly failure rate.

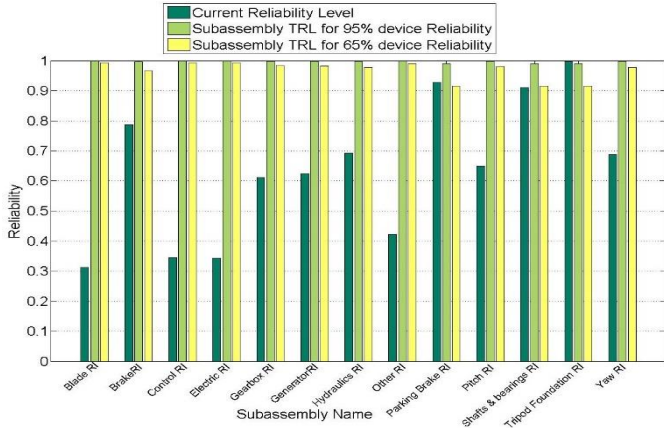


Figure 8. Actual and target reliability levels (95% and 65% device reliability) at subassembly level for RI.

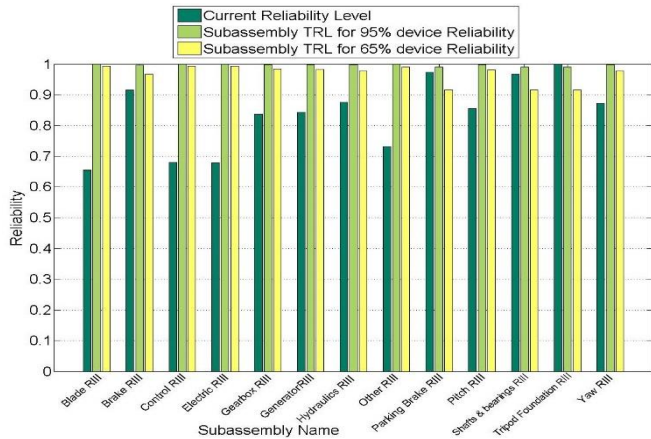


Figure 9. Actual and target reliability levels (95% and 65% device reliability) at subassembly level for RIII.

It can be seen that in order to achieve even a minimal device target reliability level of 65% requires a reliability in excess of 0.9 for each subassembly.

3.3 Influence of Metocean Conditions on Reliability

Comparison of subassembly reliability levels of RI and RIII (Fig. 10) shows the qualitative influence of metocean parameters on individual subassemblies. Device and subassembly reliability levels are lower for the device deployed at RI due to the applied adjustment factors that account for the more severe site conditions.

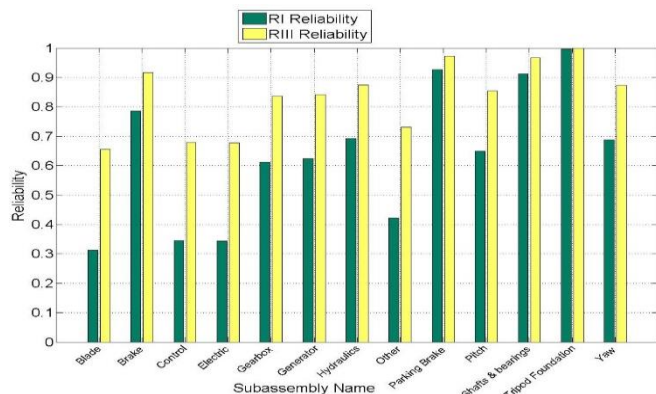


Figure 10. Subassembly reliability comparison of RI and RIII with a quarterly maintenance regime.

It is worth reiterating that the results of this case study do not provide point values for reliability since surrogate failure data and approximations of metocean conditions lead to large uncertainty bands. Instead, this study highlights the significance of translating device reliability to subassembly levels and provides indicators categorising the influence of metocean parameters on device reliability. The methodology provided can be used with high resolution, site-specific metocean data and device failure rates to improve the applicability to individual tidal energy projects.

The similarity in function and structure of onshore wind turbines and TSDs is significant, however, failure databases for the former have limited usefulness for reliability assessments of the latter. This is because placing proven equipment in the dynamic marine environment, with significantly altered load conditions and duty cycles, implies large changes in failure rates, modes and mechanisms.

Furthermore, weightage for reliability improvement was also devised based on the proportion of failure rates which leads to greater uncertainty in the results. Realising that the purpose behind device optimisation is a decrease in LCoE leads to the conclusion that subassembly maintenance costs must be factored into the equation for a more pragmatic assessment of target reliability levels. These targets can be realised by technological improvement of the individual subassemblies or introduction of redundancy in the system where possible

Metocean data with high temporal and spatial resolution is most suitable to determine the energy capture of TSDs. This is because site-specific tidal conditions differ considerably from the widely-used regional average. Also, the output of TSDs depends non-linearly on the tidal speed at every moment in time, which is very poorly captured by its regional average over a season. Similarly, the limited resolution of the metocean dataset used in this study leads to another source of error in the quantification of reliability point values. In-situ data or high resolution model data are required to address this limitation. However, the problem of the correlation between failure rate and metocean conditions cannot be resolved unless device-specific technical, operational, maintenance and failure data is provided in conjunction with metocean parameters.

Despite these limitations, the paper shows that the reliability of subassemblies must be comparatively high in order to achieve the anticipated target reliabilities, which would in turn ensure sufficiently high availability factors. It is also likely that the reliability of subassemblies will differ across the various tidal energy sites. Hence, a more refined, site specific reliability modelling is useful to explore required target reliabilities that can inform the crucial availability and capacity factors for tidal energy projects.

5 REFERENCES

- ABPmer. 2008. Atlas of UK Marine Renewable Energy Resources : Technical Report.
- Carbon Trust & Black & Veatch. 2011. UK Tidal Current Resource and Economics Study.
- Carroll, J. McDonald, A. & McMillan, D. 2015. Failure rate , repair time and unscheduled O & M cost analysis of offshore wind turbines. *Wind Energy*.
- CATAPULT. 2015. Report 3: Optimum Electrical Array Architectures. *Marine Energy Electrical Architecture*.
- Delorm, T., & Tavner, P. J. (2010). Reliability Prediction Models for Tidal Stream Devices, *20(4)*, 2010.
- T. M. 2014. Tidal Stream Devices: Reliability prediction models during their conceptual & development phases.
- Douglas, C. A. Harrison, G. P. & Chick, J. P. 2008. Life cycle assessment of the Seagen marine current turbine. *Proceedings of the Institution of Mechanical Engineers Vol. 222 Part M: J*.
- Energy Technologies Institute. 2015. Tidal Energy - Insights into Tidal Stream energy.
- Faulstich, S. & Hahn, B. 2009. Comparison of different wind turbine concepts due to their effects on reliability.
- Faulstich, S. Hahn, B. Lyding, P. & Tavner, P. J. 2009. Reliability of offshore turbines – identifying risks by onshore experience. *Wind Energy*.
- Fraenkel, P. L. 2002. Power from Marine Currents. *Proceedings of the Institution of Mechanical Engineers Vol 216 Part A : J*
- International Electrotechnical Commission. 1990. International Electrotechnical Vocabulary (IEV). *IEC 50(191)*.
- International Standardisation Organisation. 1986. Quality Vocabulary. *ISO 8402*.
- Kettle, A. 2013. Review of Met-Ocean Data for Offshore Wind Energy.
- MeyGen. 2011. MeyGen Phase 1 EIA Scoping Document.
- OGP. 2010. Structural risk for offshore installations.
- OREDA. 2002. Offshore Reliability Data.
- Rausand, M. & Høyland, A. System Reliability Theory: Models, Statistical Methods, and Applications. *2nd Edition*.
- RenewableUK. 2013. Wave and Tidal Energy in the UK: Conquering Challenges, Generating Growth.
- Strategic Initiative for Ocean Energy. 2014. Wave and Tidal Energy Market Deployment Strategy for Europe.
- Tavner, P. J. Bussel, G. J. W. Spinato, F. 2006. Machine and Converter Reliabilities in Wind Turbines. International Conference on Power Electronics, Machines and Drives.
- Tavner, P. J. Faulstich, S. Bussel, G. J. W. Koutoulakos, E. 2008. Reliability of Different Wind Turbine Concepts with Relevance to Offshore Application.
- The Crown Estate. 2013. UK Wave and Tidal Key Resource Areas Project - Technical Methodology Report.
- The Crown Estate & Black & Veatch Ltd. 2012. UK Wave and Tidal Key Resource Areas Project – Summary Report.
- Thies, P. J. Flinn, J. Smith, G. H. (2009) Is it a showstopper? Reliability Assessment and criticality analysis for Wave Energy Converter.
- United States Military. 1949. Procedure for Performing a Failure Mode Effects and Criticality Analysis.